

Prediction of Element Transfer in Submerged Arc Welding

Several studies were conducted to better understand the chemical behavior of fluxes in order to control weld metal chemistry

BY P. KANJILAL, T. K. PAL, AND S. K. MAJUMDAR

ABSTRACT. The transfer of elements across the molten weld pool has been predicted by developing quadratic models in terms of flux ingredients with the application of statistical experiments for mixture design. Bead-on-plate weld deposits were made at fixed welding parameters using submerged arc welding fluxes prepared as per extreme vertices algorithm of mixture experiments in a CaO-MgO-CaF₂-Al₂O₃ flux system. The results show that some of the individual flux ingredients and their binary mixtures have a predominant effect on weld metal transfer of oxygen, manganese, silicon, and carbon contents.

The analysis of experimental data also indicates that transfer of oxygen is affected by several properties of flux ingredients such as oxygen potential, thermodynamic stability, and viscosity. In the element transfer of silicon, both thermochemical and electrochemical reaction mechanisms operate simultaneously. Transfer of manganese is principally related to the weld metal oxygen contents as well as electrochemical reaction in the molten weld pool. The transfer of carbon was generally governed by the oxidation reaction. Iso-response contour plots were also developed to quantify the transfer of elements against different flux compositions.

Introduction

Submerged arc fluxes play a very complex role during the welding process. Besides protecting the weld pool and influencing the bead geometry, fluxes also melt in a specific temperature range, refine the weld metal, as well as take part in slag-metal reaction (Refs. 1–4) before finally being removed as slag. Several studies were carried out to understand the chem-

ical behavior of fluxes in order to control the weld metal chemistry (Refs. 4–13). Furthermore, physical properties such as viscosity, fluidity, etc. have also been reported to have pronounced effects on weld metal chemistry (Refs. 14–16). Significant interaction effect of the flux ingredients on weld metal chemistry has also been reported by previous investigators (Ref. 10).

It is well established that submerged arc welding (SAW) fluxes consisting of easily reduced oxides are the main source of weld metal oxygen. The behavior of flux has been characterized in terms of basicity index, which, however, could be considered only as a rough guide for an engineer (Ref. 1), as it fails to address the fundamental question of transfer of oxygen from flux to weld, as well as the extent of slag metal reaction in the molten weld pool (Refs. 10, 11, 13, 17, 18). Later, oxygen potential, representing the driving force for oxygen transfer from flux to weld metal was observed to facilitate better prediction of flux behavior (Ref. 5). Again, the stability of flux ingredients based on free energy of formation has been shown to be altered in the presence of welding plasma (Refs. 6, 14). Detailed studies have revealed that along with thermochemical reactions of flux, electrochemical reactions also have a significant effect on weld metal chemistry (Refs. 17, 19–22). Therefore, final weld metal chemistry is based on the integration of all possible mechanisms operating within the molten weld pool.

In general, the final weld metal composition for a particular element is made up of contributions from the filler metal, flux, and base metal. The nominal composition of each weld is calculated considering just the dilution effect (Refs. 3, 23–25). The extent of loss or gain of a specific element is evaluated by a quantity called “delta,” which is the difference between the analytical and nominal composition (Refs. 23, 25). These quantities are an indication of the influence of flux on the element transfer behavior during the SAW process (Refs. 2, 3). Therefore, in order to obtain the desired weld metal composition, it is very necessary to understand and control the flux ingredients governing the weld metal delta quantities.

In this paper, an attempt has been made to find out the quantitative effects of individual flux ingredients and their interactions on the weld metal transfer of elements in terms of delta quantities, with the application of statistical experiments for mixture design, in particular, “extreme vertices mixture design,” where the flux ingredients were varied simultaneously in CaO-MgO-CaF₂-Al₂O₃ flux systems. The aim is to develop satisfactory regression models involving proportions of flux ingredients and transfer of elements as shown in Fig. 1, so that the fluxes can be effectively used to achieve a desired level of weld metal chemical composition.

Planning of the Experiments

Extreme Vertices Design Algorithm

In experiments using a mixture of q components, a component (i^{th}) is expressed as a fraction x_i of the total mixture and the response is a function of the proportions of x_i , $i = 1, 2, \dots, q$, of the components and not the total amount of the mixture (Ref. 26). In practice, physical and chemical consideration often imposes lower (a_i) and upper (b_i) bounds $0 \leq a_i \leq x_i \leq b_i \leq 1.0$; $i = 1, 2, \dots, q$, on the levels of all of the components of the mixture.

The extreme vertices design that was used for experimentation (Refs. 26–28)

KEYWORDS

Submerged Arc Welding
Mixture Design Experiment
Extreme Vertices Algorithm
Element Transfer
Flux Ingredients
Binary Synergism
Binary Antagonism
Oxidation Loss
Electrochemical Reaction

P. KANJILAL (pra_kanjil@yahoo.co.in) is Scientist, Mechanical Eng. Div., National Test House, Salt Lake, Kolkata, India. T. K. PAL (t_k_pal@yahoo.com) is Professor, Metallurgical Eng. Dept., Jadavpur University, Kolkata, India. S. K. MAJUMDAR (skm@isical.ac.in) is Professor, SQC & OR Division, Indian Statistical Institute, Kolkata, India.

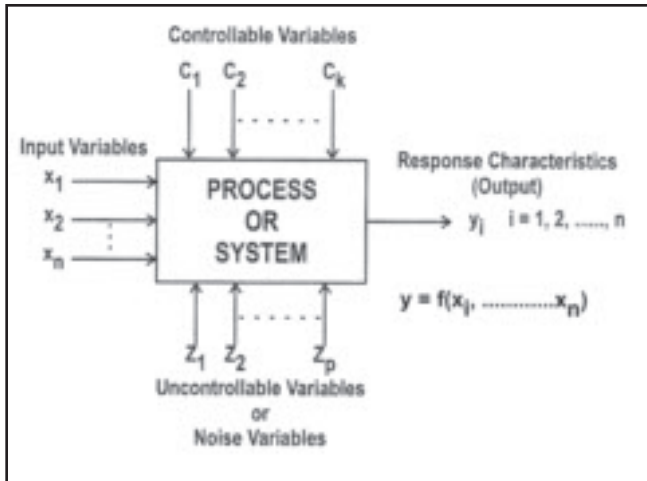


Fig. 1 — General model of a process or system in a statistical mixture design experiment.

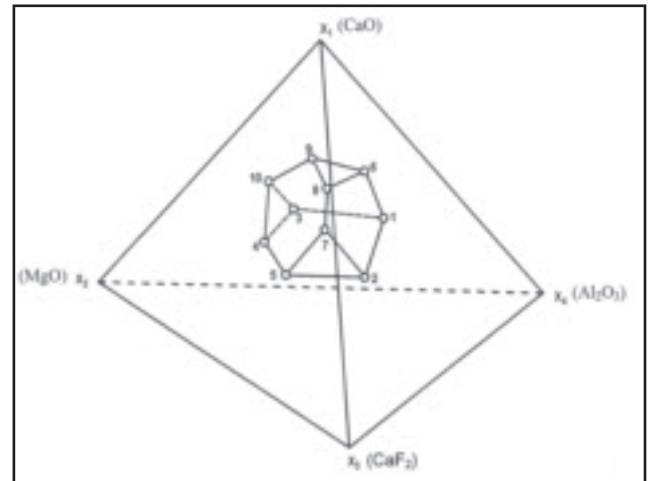


Fig. 2 — The constrained factor space inside the tetrahedron describing the experimental space.

Table 1 — Working Range of Flux Ingredients (Mixture Variable)

Flux Ingredients	Lower (wt-%)	Upper (wt-%)
Calcium oxide (CaO)	15	35
Magnesium oxide (MgO)	10	40
Calcium fluoride (CaF ₂)	10	40
Aluminium oxide (Al ₂ O ₃)	10	40

consisted of the 10 admissible vertices of the polyhedron, 7 centroids of the seven two-dimensional faces, and the overall centroid. Thus, although 10 coefficients of the quadratic regression model for the response characteristics were required to be estimated, 18 design points were deliberately chosen for getting better estimates of the coefficients and error. The above design was obtained by following the two step procedures of Mclean and Anderson (Ref. 26). After having generated $4 \times 2^{4-1} = 32$ possible combinations of the four components, it was found that there were 10 admissible vertices, which satisfied the constraint for the mixture total as also the lower and upper bounds of each component proportion. The seven two-dimensional faces of the polyhedron were found by grouping the vertices of the polyhedron into groups of three or more vertices where each vertex had the same value x_i for one of the four components. Thus, the coordinates of the seven two-dimensional faces that satisfied the constraints are the design points sl. Nos. 11 to 17. The design point sl. No. 18 was the overall centroid, which was the average of all the 10 vertices. The transpose $(x'x)^{-1}$, where x represents the complete design matrix of the given de-

Table 2 — Design Matrix of Flux Used in the Experiment at Fixed Welding Parameters

Sample No.	Mixture Variables Composition			Constants Composition	
	CaO (wt-%)	MgO (wt-%)	CaF ₂ (wt-%)	Al ₂ O ₃ (wt-%)	SiO ₂ (wt-%)
P1	15.00	15.00	10.00	40.00	10.0
P2	15.00	15.00	40.00	10.00	10.0
P3	15.00	32.40	10.00	22.60	10.0
P4	15.00	17.00	40.00	8.00	10.0
P5	15.00	32.40	24.60	8.00	10.0
P6	35.00	15.00	10.00	20.00	10.0
P7	17.00	15.00	40.00	8.00	10.0
P8	35.00	15.00	22.00	8.00	10.0
P9	29.60	32.40	10.00	8.00	10.0
P10	35.00	27.00	10.00	8.00	10.0
P11	24.43	23.14	24.43	8.00	10.0
P12	15.67	15.67	40.00	8.66	10.0
P13	25.92	24.36	10.0	19.72	10.0
P14	23.40	15.00	24.40	17.20	10.0
P15	19.87	32.40	14.86	12.87	10.0
P16	15.00	22.36	24.92	17.72	10.0
P17	35.00	19.00	14.00	12.00	10.0
P18	22.67	21.63	21.63	14.07	10.0

N.B.: Other additions to 18 flux samples. Fe-Mn = 4.0 wt-%, Fe-Si = 3.0 wt-%, bentonite = 3.0 wt-%

Table 3 — Chemical Compositions of Base Metal and Filler Metal Used for 18 Weld Metal Samples (P1-P18)

Sample	C (wt-%)	Mn (wt-%)	Si (wt-%)	S (wt-%)	P (wt-%)	O ₂ (ppm)
Base metal	0.22	0.77	0.252	0.03	0.02	350
Filler metal	0.102	0.561	0.05	0.022	0.011	380

sign, was also small. In three-dimensional space, the constraint design region is shown in Fig. 2, which represents the mixture space in the present experiment.

Snee (Ref. 29) also gave the algorithm for selecting the subsets of extreme vertices for fitting quadratic models of the following form in the constrained mixture spaces.

$$y = \sum_{i=1}^q \beta_i x_i + \sum_{i < j} \sum_{i < k} \beta_{ijk} x_i x_j x_k \quad (1)$$

The regression coefficients β_i and β_{ij} are the least square estimates in the fitted model and y is the response variable.

The percentage variation of a given response characteristic is measured by the

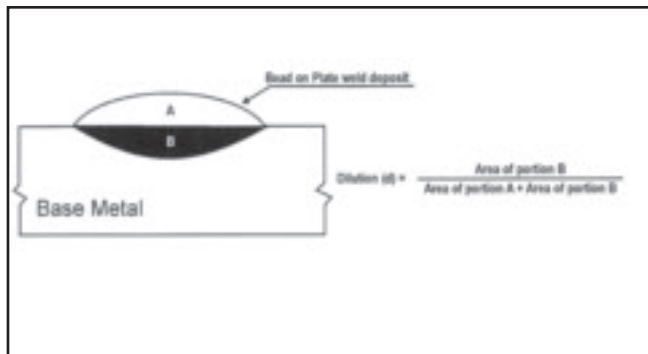


Fig. 3 — Schematic of weld deposit showing measurement of dilution.

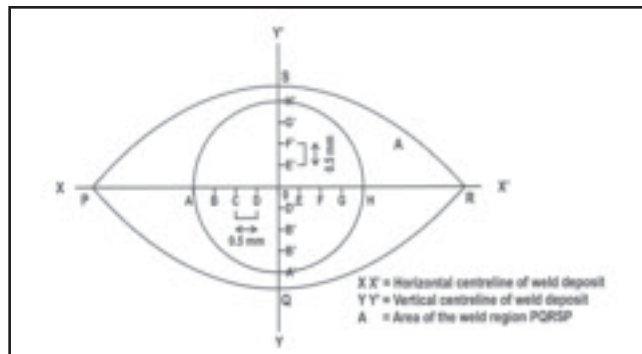


Fig. 4 — Weld metal region for EPMA analysis (shown within the circular area).

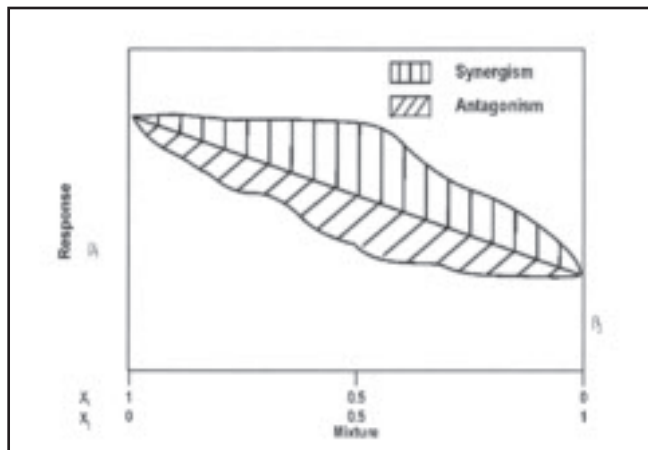


Fig. 5 — Synergism and antagonism of binary mixtures.

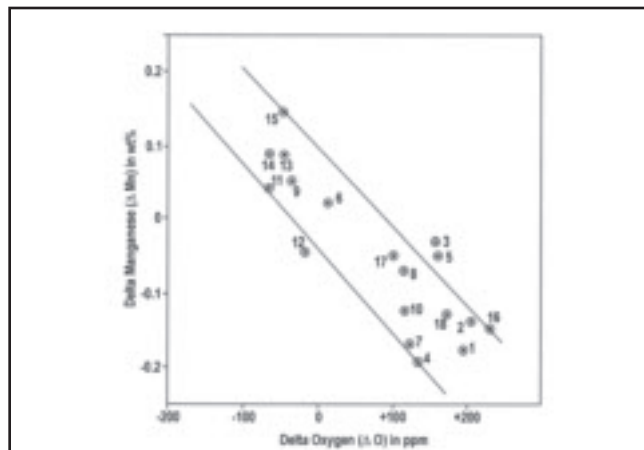


Fig. 6 — Variation of weld metal delta manganese with delta oxygen content.

term 'R', which is evaluated from the relation

$$R^2 = 1 - \frac{SSE/(N-P)}{SST/(N-1)} \quad (2)$$

Where, N is total number of observations, P is number of parameters, SSE is sum of square of errors, and SST is total sum of square.

Experimental Procedure

Formulation of Submerged Arc Fluxes

In the present study, the main aim was to investigate the effects of flux ingredients such as CaO, MgO, CaF₂, and Al₂O₃ on the transfer of metal during submerged arc welding. In order to prepare fluxes as per statistical design of experiments for mixture, the working range of each variable flux ingredient was found out by trial runs. Each ingredient viz CaO, MgO, CaF₂, and Al₂O₃ was varied from 5 to 50% at increments of 5%, with corresponding adjustment in other ingredients for each trial agglomerated flux. In the trial experiments, these fluxes were then used in making bead-on-plate weld deposits at

prefixed welding parameters of 400 A, 26 V and 4.64 mm/s speed. After completion of each weld deposit, it was inspected at low magnification (5X) for any weld defects. In addition, slag detachability was also observed. The range of each flux ingredient, where satisfactory weld deposits were obtained, was noted. The working range of each variable of flux ingredients (CaO, MgO, CaF₂, Al₂O₃) for satisfactory weld deposits is given in Table 1. Within this working range, the agglomerated fluxes used in the actual experiment were prepared from the flux ingredients, as per formulations developed by statistical experiments for mixture design. The details of 18 fluxes are given in Table 2.

Submerged Arc Welding

Single pass, bead-on-plate weld deposits were made with direct current electrode positive (DCEP) polarity using 18 experimental fluxes (Table 2) on 16-mm-thick low-carbon steel plate with 3.15-mm-diameter low-carbon steel welding wire. The parameters used during welding of these 18 samples were maintained as the same as that used during standardization of experiments on fluxes.

Chemical Composition Analysis

The chemical compositions of steel plate and welding wire are given in Table 3. Chemical compositional analysis of base metal, filler metal, and the weld metal for constituents such as carbon, manganese, silicon, sulfur, phosphorus, and nickel contents were analyzed by optical emission spectra (OES) method. Weld metal oxygen and nitrogen contents were determined by Leco interstitial analyzer. Cylindrical samples of 3-mm diameter and 9-mm length prepared by machining the weld deposits were used for oxygen and nitrogen estimates. Chemical compositions were determined at four different locations of the same weld deposits. Microphotographs were taken on the weld metal samples for measurement of weld bead parameters such as width w, transverse cross-sectional area A, and dilution d, as shown in Fig. 3.

EPMA Analysis

Transfer of elements in the weld region have been studied by electron probe micro analyzer (EPMA) for selected weld metal samples. The spot of probe analyzer on the weld bead is shown in Fig. 4.

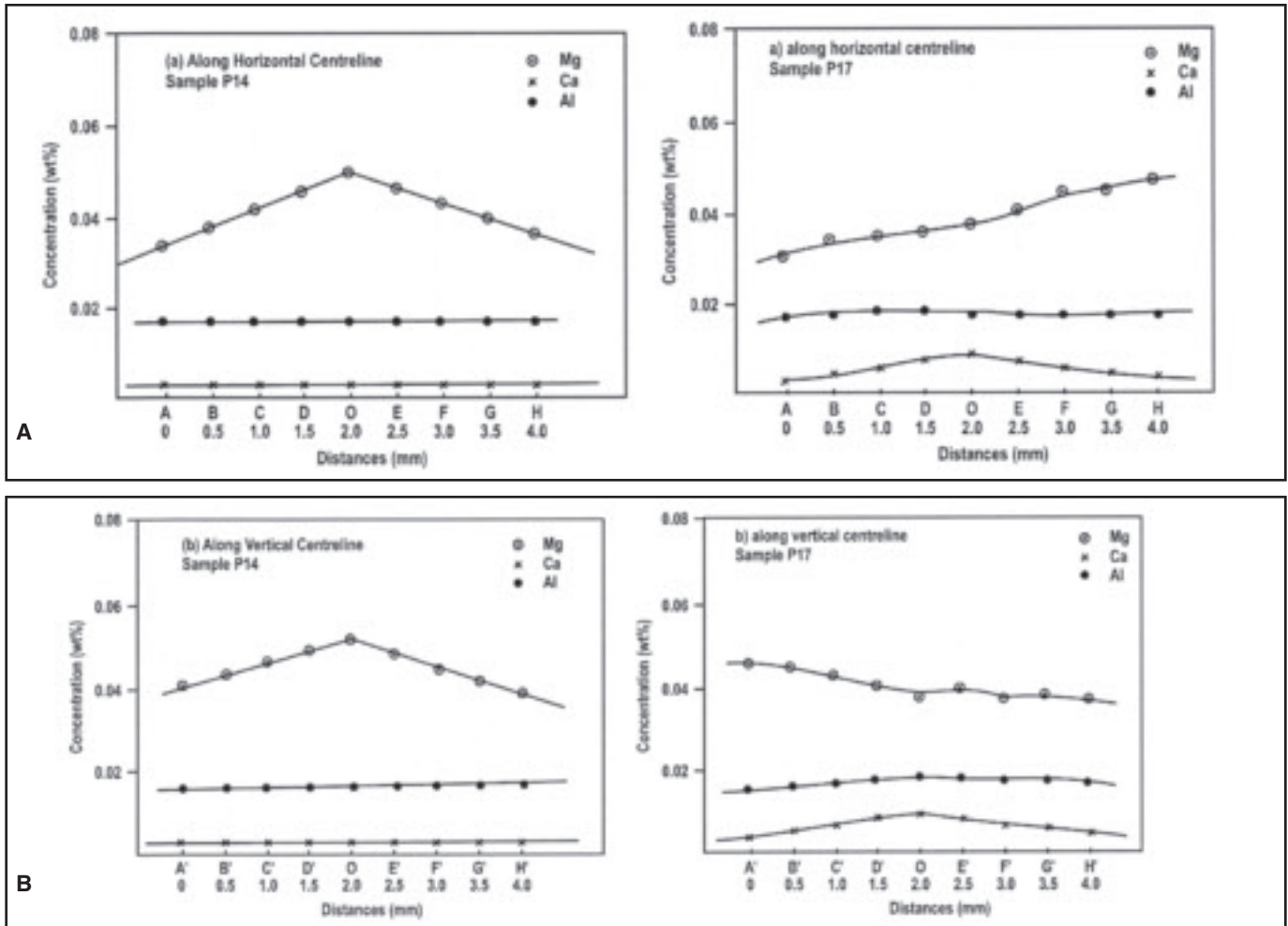


Fig. 7 — Distribution of magnesium, calcium, and aluminum along the weld metal samples P14 and P17. A — Along the horizontal centerline of the weld; B — the vertical centerline of the weld.

Results

The final weld metal composition is generally made of contributions from the welding electrodes, the base metal, and the molten metal-flux (slag-metal) reactions (Ref. 23). In the present experiment, welding parameters were not varied and flux height was kept on the base metal to a height of 0.35 mm along the path of the nozzle. Furthermore, the ratio of flux to wire melted varied within the small zone, i.e., 1.85 to 2.05. Therefore, the composition changes affected by the ratio of flux to wire melted may be assumed to be small in magnitude.

The chemical behavior of flux on element transfer is expressed in terms of a quantity delta (Δ), which is the difference between the composition of a particular element determined analytically and the amount of that element that could be present in the weld, if no elemental transfer for the weld pool to the flux or vice versa has taken place (Refs. 22, 24). This has been accomplished by taking the effect of

dilution (d), which is the ratio of base plate to weld metal melted. The dilution of 18 welded samples is given in Table 4. Since the aim of the present experiment was to study the effect of flux ingredients on element transfer, the delta quantities were considered for further analysis and discussion. Chemical compositions were determined at four different positions of the weld and delta quantities were measured corresponding to the four sets of chemical constituents. These four sets of chemical constituents and corresponding weld metal delta quantities are given in Table 5A and B, respectively.

Development of Prediction Equations for Weld Metal Elemental Transfer

Extreme vertices design algorithm (XVERT) were applied on the experimentally determined values of responses, viz. weld metal delta oxygen (ΔO), delta manganese (ΔMn), delta silicon (ΔSi), delta sulfur (ΔS), and delta carbon (ΔC) as given in Table 5B in order to develop

prediction equations for the responses. The predictors are the flux ingredients such as CaO, MgO, CaF₂, and Al₂O₃, and their binary mixture eg. CaO-MgO, CaO-CaF₂, CaO-Al₂O₃, MgO-CaF₂, MgO-Al₂O₃, and CaF₂-Al₂O₃.

The prediction equations are as follows:

$$\begin{aligned} \Delta O_2 = & 58.9318 \text{ CaO} - 17.2406 \text{ MgO} \\ & + 2.6522 \text{ CaF}_2 + 12.7800 \text{ Al}_2\text{O}_3 - 0.9086 \\ & \text{CaO.MgO} - 1.5406 \text{ CaO.CaF}_2 \\ & - 2.0416 \text{ CaO.Al}_2\text{O}_3 + 0.8562 \text{ MgO.} \\ & \text{CaF}_2 + 0.7966 \text{ MgO.Al}_2\text{O}_3 + 0.3661 \\ & \text{CaF}_2.\text{Al}_2\text{O}_3. \end{aligned} \quad (3)$$

$$\begin{aligned} \Delta Mn = & -0.029867 \text{ CaO} + 0.05574 \text{ MgO} \\ & - 0.004323 \text{ CaF} - 0.002228 \text{ Al}_2\text{O}_3 \\ & - 0.000474 \text{ CaO.MgO} + 0.001225 \text{ CaO.} \\ & \text{CaF}_2 + 0.001361 \text{ CaO.Al}_2\text{O}_3 \\ & - 0.001352 \text{ MgO.CaF}_2 - 0.001532 \\ & \text{MgO.Al}_2\text{O}_3 + 0.000204 \text{ CaF}_2.\text{Al}_2\text{O}_3 \end{aligned} \quad (4)$$

$$\begin{aligned} \Delta Si = & 0.012176 \text{ CaO} + 0.055635 \text{ MgO} \\ & + 0.006303 \text{ CaF}_2 + 0.013559 \text{ Al}_2\text{O}_3 \\ & - 0.001364 \text{ CaO.MgO} - 0.000063 \\ & \text{CaO.CaF}_2 - 0.000190 \text{ CaO.Al}_2\text{O}_3 \end{aligned}$$

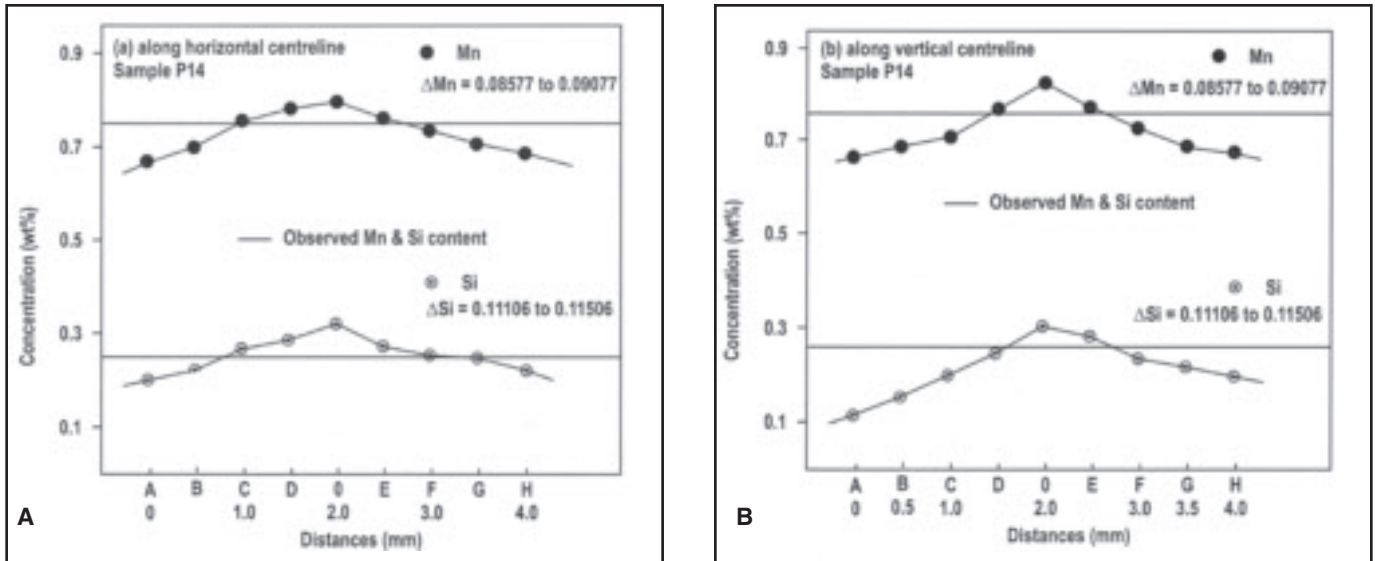
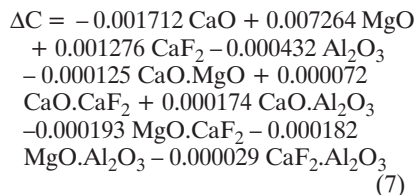
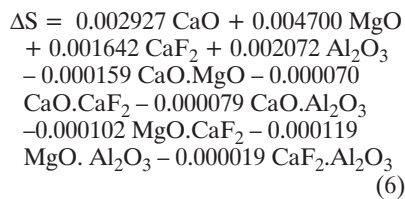
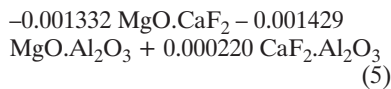


Fig. 8 — Distribution of manganese and silicon in weld metal sample P14. A — Along horizontal centerline of the weld; B — along the vertical centerline of the weld.



The model summary, coefficients, and level of significance of regression models are given in Appendices 1 and 2.

Nature of Variation of Weld Metal Delta Quantities with the Flux Ingredients

It is observed from the above prediction results (Equations 3–7) that flux ingredients have two types of effect on weld metal delta quantities, viz. 1) individual effect (x_i), and 2) interaction effect of binary mixtures ($x_i x_j$). It is to be noted here that for each response characteristics in the prediction equations developed by the regression model, only statistically significant variables and/or their binary synergism and/or binary antagonism will be considered to have a predominant effect on the given response characteristics. The concept of binary synergism and antagonism is quite different from the individual effect. The binary synergism/antagonism implies that the response value (weld

metal delta quantities) obtained due to binary mixture is more than/less than the average of that response produced by two pure ingredients forming the same binary mixture. This is shown schematically in Fig. 5. The positive sign of the coefficients of individual flux ingredient in the prediction Equations 3 to 7 implies a gain of elements from flux to weld metal, and the negative sign implies a loss of elements from weld to slag. Similarly, a positive sign of the coefficients of binary flux mixtures on each response (i.e. binary synergism) implies a gain of elements from flux to weld, and the opposite effect (binary antagonism) implies a loss of elements from weld metal to slag. Among the flux ingredients, only those ingredients and/or their binary synergic/antagonism are considered significant, when their corresponding values given in the last column (sign) of the tabular form of coefficients (under Appendixes 1 and 2) are nearly equal to 0.05 (equivalent to 95% confidence level). The statistically significant variables for flux ingredients and their binary synergism/antagonism equivalent to 95% confidence level are summarized in Table 6. The other nonsignificant variables, although they constitute a part of the prediction equations, were not considered to have predominant effect on the response because these effects were not distinguishable from the random noise generated in the experiments.

Finally, the prediction equation for the response delta sulfur (ΔS) (Equation 6) is not a good fit as evident from R^2 values, given in Appendixes 1 and 2, and hence, this response is not considered for detailed discussion. However, the effect of each flux ingredient and its binary mixtures are stated in Table 6.

Table 4 — Dilution for 18 Weld Metal Samples in Model 1 Experiment at Fixed Welding Parameters

Sample No.	Dilution (d)	1-d
P1	0.41	0.59
P2	0.47	0.53
P3	0.45	0.55
P4	0.47	0.53
P5	0.43	0.57
P6	0.43	0.57
P7	0.46	0.54
P8	0.43	0.57
P9	0.39	0.61
P10	0.49	0.51
P11	0.47	0.53
P12	0.41	0.59
P13	0.46	0.54
P14	0.47	0.53
P15	0.45	0.55
P16	0.46	0.54
P17	0.42	0.58
P18	0.43	0.57

Discussion

The transfer of elements across the weld pool in submerged arc welding is attributed to the combined actions of several reactions that take place simultaneously in the molten weld pool. It has already been stated (Refs. 1–4, 19) that physical as well as chemical properties of fluxes are responsible for the transfer of elements in submerged arc welding. Among the transfer of elements in these studies, oxygen is the most important element of concern, because, beside its effect on the transfer of other elements like manganese, silicon, carbon, etc., oxygen in weld metal has a significant effect on weld metal microstructure and mechanical properties.

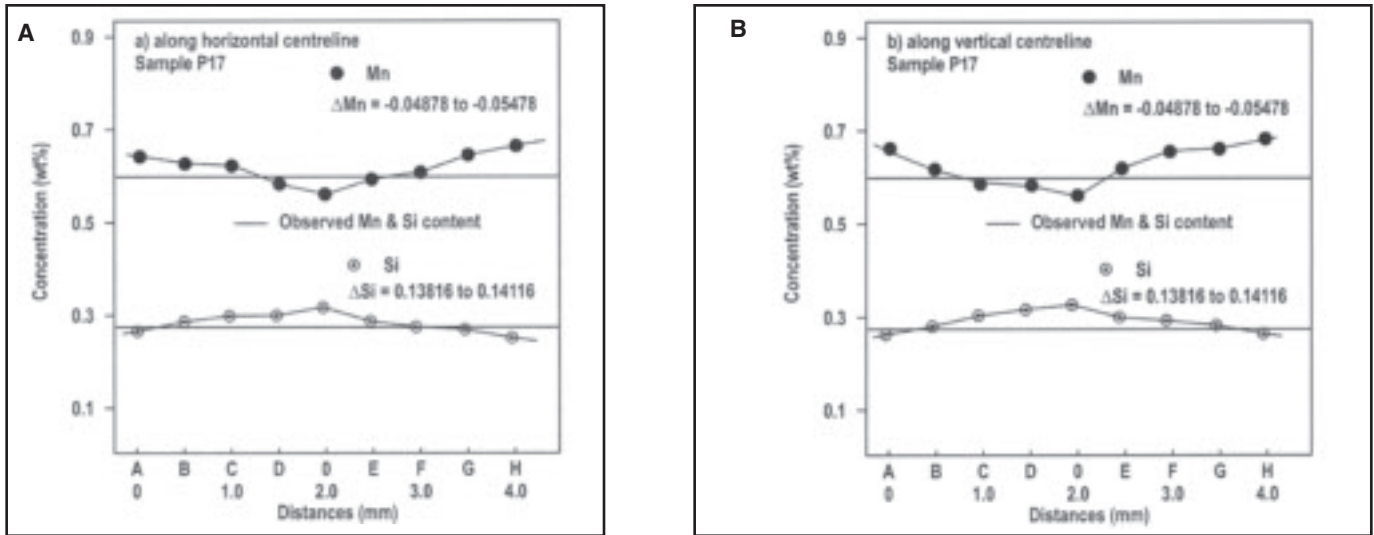


Fig. 9 — Distribution of manganese and silicon nickel in weld metal sample P17. A — Along horizontal centerline of the weld; B — along the vertical centerline of the weld.

Table 5a — Chemical Composition of 18 Weld Metal Samples at Four Different Locations of the Weld Deposits

Sample No.	Oxy (ppm)	Oxy (ppm)	Oxy (ppm)	Oxy (ppm)	Mn (wt-%)	Mn (wt-%)	Mn (wt-%)	Mn (wt-%)	Si (wt-%)	Si (wt-%)	Si (wt-%)	Si (wt-%)
P1	560	555	557	550	0.56	0.563	0.55	0.558	0.340	0.337	0.341	0.341
P2	568	563	564	558	0.52	0.522	0.521	0.524	0.21	0.211	0.212	0.208
P3	524	525	515	516	0.62	0.624	0.622	0.614	0.28	0.282	0.281	0.282
P4	500	496	505	490	0.47	0.468	0.466	0.478	0.17	0.169	0.173	0.174
P5	528	524	526	520	0.6	0.588	0.594	0.595	0.248	0.244	0.245	0.243
P6	380	370	377	375	0.67	0.673	0.674	0.672	0.229	0.227	0.228	0.230
P7	488	486	482	480	0.488	0.49	0.494	0.485	0.27	0.269	0.271	0.265
P8	481	482	476	484	0.58	0.583	0.582	0.581	0.2	0.202	0.201	0.202
P9	332	335	338	343	0.69	0.691	0.693	0.685	0.26	0.262	0.264	0.257
P10	484	470	477	468	0.54	0.541	0.539	0.536	0.193	0.195	0.191	0.190
P11	300	306	306	310	0.7	0.702	0.703	0.710	0.12	0.124	0.124	0.122
P12	352	351	348	360	0.601	0.6	0.601	0.610	0.15	0.153	0.15	0.153
P13	319	327	323	330	0.62	0.624	0.619	0.614	0.16	0.163	0.159	0.156
P14	302	310	300	316	0.748	0.745	0.75	0.750	0.258	0.256	0.255	0.260
P15	320	315	318	314	0.8	0.806	0.803	0.798	0.37	0.368	0.372	0.364
P16	595	594	593	590	0.507	0.509	0.505	0.502	0.2	0.204	0.203	0.205
P17	468	475	470	482	0.595	0.596	0.594	0.600	0.273	0.273	0.274	0.276
P18	541	530	545	525	0.517	0.513	0.519	0.516	0.16	0.161	0.163	0.168

Table 5a — Continued

Sample No.	S (wt-%)	S (wt-%)	S (wt-%)	S (wt-%)	C (wt-%)	C (wt-%)	C (wt-%)	C (wt-%)
P1	0.042	0.038	0.04	0.040	0.07	0.068	0.069	0.067
P2	0.042	0.04	0.042	0.039	0.07	0.071	0.068	0.068
P3	0.04	0.036	0.041	0.042	0.07	0.07	0.071	0.073
P4	0.034	0.036	0.033	0.036	0.06	0.061	0.062	0.059
P5	0.044	0.044	0.046	0.041	0.068	0.067	0.07	0.065
P6	0.028	0.028	0.03	0.030	0.098	0.096	0.095	0.093
P7	0.04	0.043	0.039	0.037	0.072	0.076	0.072	0.070
P8	0.028	0.03	0.03	0.026	0.07	0.069	0.078	0.072
P9	0.027	0.025	0.027	0.026	0.068	0.070	0.069	0.070
P10	0.034	0.033	0.034	0.030	0.063	0.067	0.066	0.060
P11	0.021	0.022	0.023	0.025	0.073	0.072	0.074	0.075
P12	0.037	0.035	0.036	0.034	0.095	0.092	0.091	0.091
P13	0.016	0.018	0.018	0.020	0.084	0.08	0.082	0.085
P14	0.031	0.029	0.032	0.030	0.089	0.085	0.087	0.091
P15	0.02	0.022	0.023	0.025	0.094	0.095	0.093	0.092
P16	0.024	0.025	0.027	0.027	0.061	0.062	0.059	0.057
P17	0.015	0.016	0.018	0.021	0.082	0.082	0.082	0.078
P18	0.023	0.023	0.025	0.022	0.058	0.057	0.055	0.060

Transfer of Oxygen

The positive and negative values of delta oxygen as given in Table 5B indicate both gain and loss of oxygen in weld metal had taken place during welding. The summarized results in Table 6 show that flux ingredients CaO and Al₂O₃ resulted in gain of oxygen for flux to weld metal. However, all binary mixtures of CaO viz. CaO-CaF₂, CaO-Al₂O₃, and CaO-MgO have binary antagonistic effect i.e., which means in all three cases, a loss of oxygen has taken place. Although CaO is considered to be a stable oxide (Ref. 23), the other characteristics of CaO, such as hygroscopic nature and reduction in viscosity of the slag (Refs. 2, 6, 14, 15, 24), increase the chances of contamination with air and moisture, which might be respon-

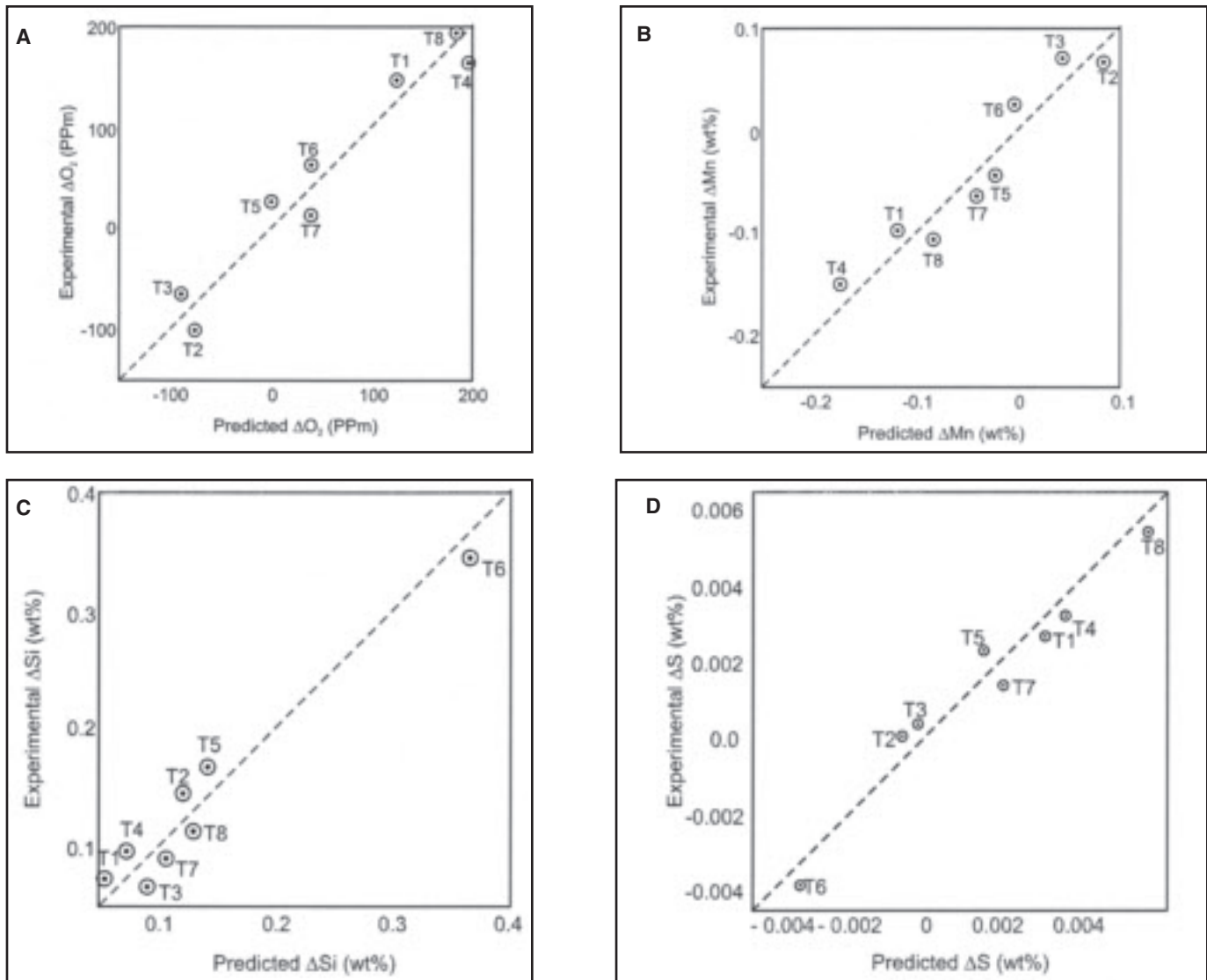
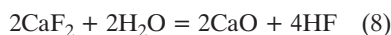


Fig. 10 — Comparison between experimental and predicted results for weld metal delta (Δ) quantities. A — ΔO_2 ; B — ΔMn ; C — ΔSi ; D — ΔS .

sible for an increase in oxygen content in the weld. The other flux ingredient Al_2O_3 can increase the oxygen content by liberating oxygen into the weld pool by suboxide formation (Ref. 6).

However, for the binary mixture of CaO, it is important to mention that CaF_2 being a nonoxide reduces the oxygen level by diluting the oxygen active species (Ref. 6). CaF_2 also increases viscosity of slag, particularly when CaO content is above 15 wt-% as observed by Mills and Keene (Ref. 15). CaF_2 may also reduce the hygroscopic nature of CaO by the following reaction:



Therefore, binary antagonistic effect of CaO- CaF_2 mixture on oxygen transfer is not unexpected. Similarly, in the case of

CaO- Al_2O_3 mixture, it is the networking capability of Al_2O_3 in basic slag that ultimately increases the viscosity of the slag (Ref. 30), resulting in minimum oxygen entrapment in the weld metal by atmospheric contamination. Furthermore, CaO may reduce the activity of Al_2O_3 through the formation of stable calcium aluminate, (Ref. 15), which will reduce the tendency of suboxide formation of Al_2O_3 . The result is lesser chance of oxygen liberation in molten weld pool by suboxide formation of Al_2O_3 . Mixture of CaO-MgO, to a lesser extent, also has a binary antagonistic (loss of oxygen) effect, as evident from its coefficient of estimate given in Equation 3. The probable reason may be that MgO is not reported to contribute oxygen in the weld by atmospheric contamination associated with reduction in viscosity. Furthermore, Mg has higher deoxidation

characteristics (Ref. 31). Therefore, with the addition of MgO to CaO, the increased deoxidation characteristics of flux reduce the oxygen content of weld metal, and thus helps to transfer oxygen from weld metal to slag.

An interesting result emerges from Table 6 that the effect of binary mixture of MgO, i.e., MgO- CaF_2 and MgO- Al_2O_3 , is opposite to that of CaO- CaF_2 and CaO- Al_2O_3 as far as transfer of oxygen is concerned. Regarding binary synergism, i.e., (gain of oxygen) by MgO- Al_2O_3 mixture, we may say that unlike CaO, MgO is not observed to decrease the activity of Al_2O_3 by formation of complex compound, since MgO- Al_2O_3 compound has a higher boiling point (2130°C) compared to the boiling point (1600°C) of CaO+ Al_2O_3 compound (Ref. 32). Therefore, activity of Al_2O_3 is not decreased and hence no such

Table 5b — Delta (Δ) Quantities of Weld Metal Constituents at Four Different Locations of Same Weld Deposit

Sample No.	ΔO_2 (ppm)	ΔO_2 (ppm)	ΔO_2 (ppm)	ΔO_2 (ppm)	ΔMn (wt-%)	ΔMn (wt-%)	ΔMn (wt-%)	ΔMn (wt-%)	ΔSi (wt-%)	ΔSi (wt-%)	ΔSi (wt-%)	ΔSi (wt-%)
P1	192.3	187.3	189.3	182.3	-0.08669	-0.08369	-0.09669	-0.08669	+0.20718	0.20418	0.20818	0.20818
P2	202.1	197.1	198.1	192.1	-0.13923	-0.13723	-0.13823	-0.13523	+0.06506	0.06606	0.06706	0.06306
P3	157.5	158.5	148.5	149.5	-0.03505	-0.03105	-0.03305	-0.04105	+0.1391	0.1411	0.1401	0.1411
P4	134.1	130.1	139.1	124.1	-0.18923	-0.19123	-0.19323	-0.18123	+0.02506	0.02406	0.02806	0.0296
P5	160.9	156.9	158.9	152.9	-0.05087	-0.06287	-0.05687	-0.05587	+0.11114	0.10714	0.10814	0.10614
P6	12.9	2.9	9.9	7.9	+0.01913	0.02213	0.02313	0.02113	+0.09214	0.09014	0.09114	0.09314
P7	121.8	119.8	115.8	113.8	-0.16914	-0.16714	-0.16314	-0.17214	+0.12708	0.12608	0.12808	0.12208
P8	113.9	114.9	108.9	116.9	-0.07087	-0.06787	-0.06887	-0.06987	+0.06314	0.06514	0.06414	0.06514
P9	-36.3	-33.3	-30.3	-25.3	+0.04749	0.04844	0.05049	0.04249	+0.13122	0.13322	0.13522	0.12822
P10	118.7	104.7	111.7	102.7	-0.12341	-0.12341	-0.12441	-0.12741	+0.04402	0.04602	0.04202	0.04102
P11	-65.9	-59.9	-59.9	-55.9	+0.04077	0.04277	0.04377	0.05077	-0.02494	-0.02094	-0.02094	-0.02294
P12	-15.7	-16.7	-19.7	-7.7	-0.04569	-0.04669	-0.04569	-0.03669	+0.01718	0.02018	0.01718	0.02018
P13	-47.2	-39.2	-43.2	-36.2	-0.03714	-0.03314	-0.03814	-0.04314	+0.01708	0.02008	0.01608	0.01308
P14	-63.9	-55.9	-65.9	-49.9	+0.08877	0.08577	0.09077	0.09077	+0.11306	0.11106	0.11006	0.11506
P15	-46.5	-51.5	-48.5	-52.5	+0.14494	0.15094	0.14794	0.14294	+0.2291	0.2271	0.2311	0.2231
P16	228.8	227.8	226.8	223.8	-0.15014	-0.14814	-0.15214	-0.15514	+0.05708	0.06108	0.06008	0.06208
P17	100.6	107.6	102.6	114.6	-0.05378	-0.05278	-0.05478	-0.04878	+0.13816	0.13816	0.13916	0.14116
P18	173.9	162.9	177.9	157.9	-0.13387	-0.13787	-0.13187	-0.13427	+0.02314	0.02414	0.02614	0.03114

Table 5b — Continued

Sample No.	Δs (wt-%)	ΔS (wt-%)	ΔS (wt-%)	ΔS (wt-%)	ΔC (wt-%)	ΔC (wt-%)	ΔC (wt-%)	ΔC (wt-%)
P1	0.01672	0.01272	0.01472	0.01472	-0.08038	-0.08238	-0.08138	-0.08338
P2	0.01624	0.01424	0.01624	0.01324	-0.08746	-0.08646	-0.08946	-0.08946
P3	0.0144	0.0104	0.0154	0.0164	-0.0851	-0.0851	-0.0841	-0.0821
P4	0.00824	0.01024	0.00724	0.01024	-0.09746	-0.09646	-0.09546	-0.099846
P5	0.01856	0.01856	0.02056	0.0156	-0.08474	-0.08574	-0.08274	-0.08774
P6	0.00256	0.00256	0.00456	0.00456	-0.05474	-0.05674	-0.05774	-0.05974
P7	0.01432	0.01732	0.01332	0.01132	-0.08428	-0.08028	-0.08428	-0.08628
P8	0.00256	0.00456	0.00456	0.00056	-0.08274	-0.08374	-0.07474	-0.08074
P9	0.00408	-0.00208	0.00408	0.00308	-0.08002	-0.07802	-0.07902	-0.07802
P10	0.00808	0.00708	0.00808	0.00408	-0.09682	-0.09282	-0.09382	-0.09982
P11	-0.00475	-0.00376	-0.00276	-0.00076	-0.08446	-0.08546	-0.08346	-0.08246
P12	0.01172	0.00972	0.01072	0.00872	-0.05538	-0.05838	-0.05938	-0.05938
P13	-0.00968	-0.00768	-0.00768	-0.00568	-0.07228	-0.07628	-0.07428	-0.07128
P14	0.00524	0.00324	0.00624	0.00424	-0.06846	-0.07246	-0.07046	-0.06646
P15	-0.0056	-0.0036	-0.0026	-0.0006	-0.0611	-0.0601	-0.0621	-0.0631
P16	-0.00168	-0.00068	-0.00132	-0.00132	-0.09528	-0.09428	-0.09728	-0.09928
P17	-0.00836	-0.00936	-0.00376	-0.00736	-0.06956	-0.06956	-0.06956	-0.07356
P18	-0.00244	-0.00244	-0.00044	-0.00344	-0.09474	-0.09574	-0.09774	-0.09274

chances of reduction of oxygen content. Regarding the mixture $CaF_2-Al_2O_3$, it is important to mention that formation of such complex compound of $CaF_2-Al_2O_3$ has not been reported, so the chances of decrease in oxygen content by complex compound formation does not arise for the mixture $CaF_2-Al_2O_3$.

Transfer of Manganese and Silicon

The manganese transfer data (ΔMn) in Table 5B show that gain in weld metal Mn (i.e., ΔMn +ve) occurs in samples P6, P9, P11, P14, and P15. Among these samples, P9, P11, P14, and P15 show loss of oxygen and sample P6 shows very low level of gain of oxygen ($\Delta = 2.9$ to 12.9 ppm). It is also pertinent to note the majority of samples that show a loss of Mn ($\Delta Mn = -ve$) also

show a gain of oxygen ($\Delta O = +ve$). This phenomenon suggests that manganese transfer is also related to the transfer of oxygen in weld metal. With the increase of oxygen transfer into the weld metal, loss of manganese in the weld metal by oxidation was also observed by previous investigators (Refs. 4, 8, 14). The variation of ΔMn with ΔO_2 in weld metal, as shown in Fig. 6, supports such observation. A close look on the summarized result in Table 6 indicates two important aspects. Flux ingredient CaO increases (gain) oxygen transfer and expectedly decreases (loss) manganese transfer in weld metal. Flux mixtures $CaO-CaF_2$ and $CaO-Al_2O_3$ have binary synergistic (gain) effect on oxygen transfer, whereas the same mixtures have binary synergistic (gain) effect on manganese transfer. The other two mixtures,

viz. $MgO-CaF_2$ and $MgO-Al_2O_3$, have reverse effects i.e., binary synergistic (gain) effect on oxygen transfer and binary antagonistic (loss) effect on manganese transfer. The relationship between ΔMn and ΔO_2 , as shown in Fig. 6, supports such behavior of flux mixtures as predicted in Table 6. Contrary to ΔMn , all samples except P11 recorded a gain of Si in the weld metal i.e. (ΔSi +ve). Since the flux system has SiO_2 as one of the constituents (10 wt-%), gain in Si (ΔSi +ve) may be possible due to the transfer of Si from flux to weld metal by thermochemical dissociation (Refs. 33, 34) and electrochemical reaction mechanism (Ref. 19). Flux ingredient Al_2O_3 may allow silicon in the flux to transfer into the weld metal by replacement of silica in silicate slag (Ref. 1).

The gain of manganese and silicon by MgO is reported in Equations 4 and 5. Table 6 may be explained by electrochemical reaction. In DCEN welding, Mg dissociates from MgO deposited at the base metal cathode by electrochemical reduction reaction of the filler metal. Manganese and silicon will form MnO and SiO_2 , respectively, and dissolve in the weld pool. Due to limited solubility in molten metal (Ref. 33), Mg will react with these oxides (MnO and SiO_2) and form again as MgO . As a result, Mn and Si are expected to increase in the weld metal. However, difficulties may arise if Ca and Al are picked up from the slag by electrochemical reaction at the cathode, since CaO and Al_2O_3 are more stable than MgO at the high temperature encountered in submerged arc welding (Ref. 20). The higher the concentration of magnesium in the weld metal, the lower are Ca and Al, as observed by EPMA studies of weld metal samples (refer to P14 and P17) shown in Fig. 7. They probably support the hypoth-

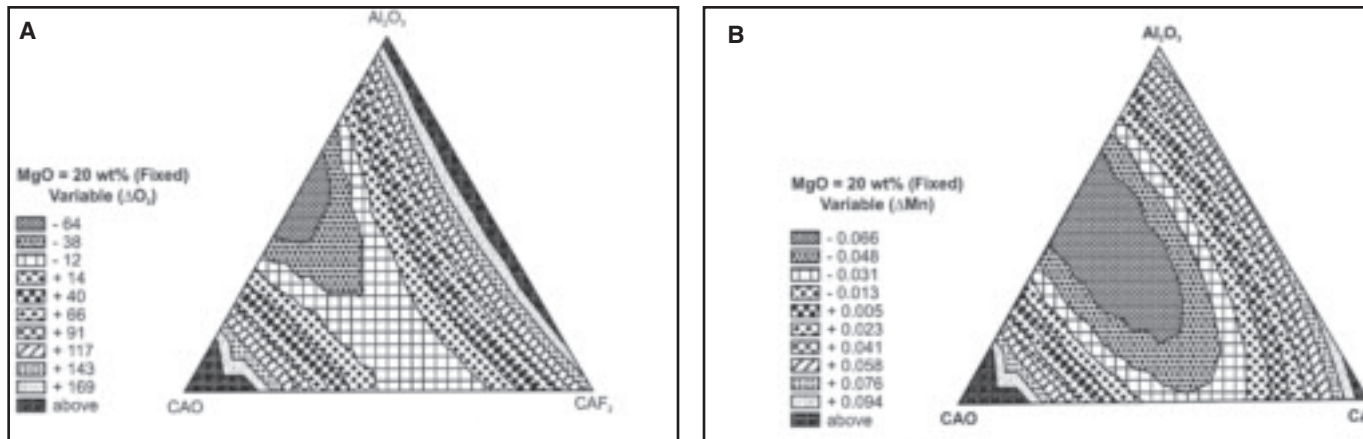


Fig. 11 — Fillet surface contour of weld metal. A — ΔO_2 ; B — ΔMn .

esis of more Mg pick-up from the slag.

It is also observed from Table 5B that sample P14 recorded a gain of Mn. The EPMA analysis of sample P14 along the horizontal and vertical centerline of weld (Fig. 8) shows maximum transfer of Mn occurs at the central region of the weld deposit. This may be due to the fact that weld metal remained liquid and solidified last, therefore giving more chances of both thermochemical and electrochemical reaction. Similarly, the maximum transfer of Si was observed for sample P14 at the central region of the weld deposit as evident in EPMA analysis silicon in Fig. 8. Interestingly sample P17 recorded loss of Mn (ΔMn from -0.04878 to -0.05478) but gain of Si (ΔSi from 0.13816 to 0.14116) as shown in Fig. 9. However, the transfer process (loss and gain) was mostly restricted along the central region of the weld deposit, similar to that observed in sample P14.

The loss of ΔMn and ΔSi by MgO-CaF₂ mixture could be justified as the addition of MgO in CaF₂ increases density and decreases conductivity of the melt (Ref. 15), which may hinder the transfer of Mn and Si across slag-metal interface. The other mixture CaO-MgO has a binary antagonistic (loss) effect on Si content. This behavior is associated with the reduction of SiO₂ activity by formation of complex silicates (Ref. 32). With the reduction of SiO₂ activity, the transfer of Si into the weld metal also decreased.

Transfer of Sulfur

The prediction results given in Table 6 show that individual flux ingredients CaO, MgO, CaF₂, and Al₂O₃ are responsible for the gain of sulfur in the weld metal. Whereas, the binary mixtures, viz. CaO-MgO, CaO-CaF₂, CaO-Al₂O₃, MgO-CaF₂, and MgO-Al₂O₃ causes loss of sulfur (desulfurization) from the weld metal. It has been observed by U. Mitra and T. W.

Table 6 — Predominant Effect of Flux Ingredients and Their Binary Mixtures on Weld Metal Delta (Δ) Quantities

(Responses) Weld Metal Delta (Δ) quantities	Predominant Effects			
	Pure Flux Ingredient Increase	Pure Flux Ingredient Decrease	Binary Mixtures of Flux Ingredient Synergism	Binary Mixtures of Flux Ingredient Antagonism
ΔO_2	CaO, Al ₂ O ₃	—	MgO-CaF ₂ , MgO-Al ₂ O ₃ , CaF ₂ -Al ₂ O ₃	CaO-MgO, CaO-CaF ₂ , CaO-Al ₂ O ₃
ΔMn	MgO	CaO	CaO-CaF ₂ , CaO-Al ₂ O ₃	MgO-CaF ₂ , MgO-Al ₂ O ₃ , CaO-CaF ₂
ΔSi	CaO, MgO, CaF ₂ , Al ₂ O ₃	—	—	MgO-CaF ₂ , MgO-Al ₂ O ₃ , CaO-MgO, CaO-CaF ₂ , CaO-Al ₂ O ₃
ΔS	MgO, CaF ₂ , Al ₂ O ₃	—	—	MgO-MgO, MgO-Al ₂ O ₃ , CaO-MgO, MgO-CaF ₂
ΔC	MgO, CaF ₂	—	CaO-CaF ₂ , CaO-Al ₂ O ₃ , MgO-CaF ₂	MgO-Al ₂ O ₃ , CaO-MgO, CaO-CaF ₂ , CaO-Al ₂ O ₃
O ₂	CaO, CaF ₂ -Al ₂ O ₃	—	MgO-Al ₂ O ₃ , CaF ₂ -Al ₂ O ₃	CaO-MgO, CaO-CaF ₂ , CaO-Al ₂ O ₃

Eagar (Ref. 8) that apart from flux basicity, type of flux also has a significant influence on sulfur transfer. In steel making, sulfur is removed by reduction reaction. Desulfurization is promoted by high-basicity and low-oxygen potential of the flux. In order to find out the effect of flux ingredients as well as their binary mixtures on weld metal oxygen content, prediction equations were developed for oxygen content as given below.

$$\begin{aligned} \text{Oxygen (O}_2 \text{ ppm)} = & 63.305 \text{ CaO} - 12.420 \text{ MgO} - 6.457 \text{ CaF}_2 - 16.775 \text{ Al}_2\text{O}_3 - 0.945 \\ & \text{CaO.MgO} - 1.557 \text{ CaO.CaF}_2 - 2.061 \\ & \text{CaO. Al}_2\text{O}_3 + 0.835 \text{ MgO.CaF}_2 + 0.767 \\ & \text{MgO.Al}_2\text{O}_3 + 0.378 \text{ CaF}_2.\text{Al}_2\text{O}_3 \quad (9) \end{aligned}$$

The predominant effects of flux ingre-

Table 7 — Randomly Designed Submerged Arc Flux Composition

Sample No.	Mixture Variables Composition			
	CaO (wt-%)	MgO (wt-%)	CaF ₂ (wt-%)	Al ₂ O ₃ (wt-%)
T1	17	20	30	13
T2	30	15	15	20
T3	25	30	15	10
T4	15	25	10	30
T5	20	28	12	20
T6	23	27	15	15
T7	19	18	11	32
T8	16	17	25	22

N.B.: Other additions to flux samples. SiO₂=10 wt-%, Fe-Mn=4.0 wt-%, Fe-Si=3.0 wt-%, bentonite=3.0.

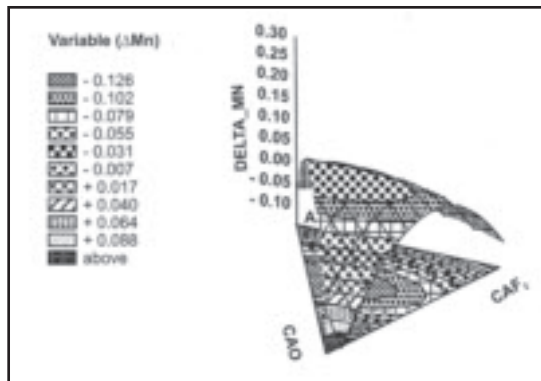


Fig. 12 — Fillet surface contour in three dimension for weld metal ΔMn .

dients and their binary mixtures are also incorporated in Table 6. The statistical details of the equations are given in Appendixes 2 and 3.

Since CaO, CaF₂, and Al₂O₃ increase weld metal oxygen content, as given in Table 6, desulfurization reaction will not be favored by these ingredients due to the reason that sulfur is removed by reduction reaction (Refs. 8, 9), therefore these three ingredients will help the gain of sulfur in the weld metal. However, MgO was not reported to increase weld metal oxygen content (Table 6). In spite of that, the gaining of sulfur by MgO indicates MgO is not capable of desulfurization. The probable reason may be 1) the radius of Mg²⁺ ions (0.78 Å) is less than that of Ca²⁺ ions (1.06 Å), 2) the stability of MgS is less than that of CaS, and 3) the solubility of desulfurization product MgS in weld metal is more than that of CaS (Ref. 34). All these phenomena probably reduce the sulfur absorbing capacity of MgO in the flux.

The loss of sulfur by CaO-MgO flux mixture (Table 6) could be due to an increase in free oxygen ion with addition of basic oxide and a decrease in the content of Fe⁺⁺ by dilution. Both of these circumstances are favorable to the desulfurization process (Ref. 35). On the other hand, loss of sulfur by flux mixtures MgO-Al₂O₃ and CaO-Al₂O₃ could be due to the formation of oxygen ion in the slag, which results in the formation of a complex compound by the reaction of aluminate ion (or silicon aluminate ion) with the sulfur ion (Ref. 35). Furthermore, since CaO-CaF₂ and CaO-Al₂O₃ mixtures decrease (binary antagonism) oxygen content (Table 6), desulfurization reactions will be favored by these two mixture also, leading to loss of sulfur in the weld metal.

Adequacy of the Developed Prediction Equation

The adequacy of the prediction equations for weld metal delta quantities was

checked by performing submerged arc welding using randomly designed fluxes — Table 7. The experimentally determined and theoretically predicted results of ΔO_2 , ΔMn , ΔSi , and ΔS are compared graphically in Fig. 10. It is observed from Fig. 10 that there is reasonably good agreement between the experimental and predicted results. Therefore, we may infer that the prediction model is quite adequate in describing weld metal delta (Δ) equation, viz. ΔO_2 , ΔMn , ΔSi , and ΔS .

Occasionally experiments are planned to be performed in some reasonably well-defined region of interest, centered about the operating conditions. The reason for exploring the region of interest is to see if there are other blends (mixture) in the vicinity of current conditions that can produce a response similar to or better than those currently being produced (Ref. 36). These response contour plots will be a useful tool for the designer in selecting the proper flux ingredient (composition) ranges in order to achieve their desired target value of that response.

The iso-response contour plots for selected responses, such as weld metal delta oxygen content and delta manganese content, were developed in the present experiment as an example. These are shown in Fig. 11A and B, respectively. The iso-response contour plots in three dimensions has been developed for the selected response (ΔMn), as shown in Fig. 12. The shades in each of these iso-response contour plots represent the value of the responses that may be achievable at different combinations of flux ingredients in the present set of experiments.

Conclusions

Following conclusions can be drawn from this study:

1) The transfer of elements, viz oxygen, manganese, silicon, and sulfur across the weld pool in submerged arc welding (SAW) can be predicted by developing suitable regression models with the help of statistical design of mixture experiments.

2) The variation of transfer of elements across the weld pool is primarily due to chemical reactions associated with SAW fluxes at fixed levels of the welding parameters.

3) Increase in viscosity by CaO and suboxide formation properties by Al₂O₃ are also the reason for oxygen transfer from flux to weld.

4) The interaction of CaO with CaF₂ and Al₂O₃ results in the loss of oxygen (re-

fining) and a gain of manganese (alloying) content in the weld metal. However, the interaction of MgO with CaF₂ and Al₂O₃ shows an opposite effect toward oxygen and manganese transfer.

5) Gain of manganese in the weld metal resulted from an electrochemical reaction in the weld pool.

6) Gain of silicon in the weld metal was due to thermochemical dissociation and electrochemical reaction in the weld pool.

7) Transfer of sulfur from weld to flux is affected by an increase in oxygen in the molten weld pool. Low carbon is mainly due to the oxidation of available oxygen in molten weld pool.

References

1. Davis, M. L. E., and Bailey, N. 1980. How submerged arc flux composition influences element transfer. *International Conference on Trends in Steels and Consumables for Welding*. The welding Institute, London, UK: Paper 34, pp. 289–302.
2. Davis, M. L. E., and Bailey, N. 1978. Have we the right ideas about fluxes? *Proceedings of the International Conferences on Trends in Steels and Consumables for Welding*. The Welding Institute, London, UK: Paper 19, pp. 231–247.
3. Olson, D. L. 1989. Keynote address. The fundamentals of welding consumables. *Proceedings of the 2nd International Conference on Trends in Welding Research*, Gattlinburg, Tenn., pp. 551–562.
4. Davis, M. L. E., and Coe, F. R. 1977. The chemistry of submerged arc welding fluxes. The Welding Institute Research Report: 39/1977/M, May, pp. 1–61.
5. North, T. H., Bell, H. B., Nowicki, A., and Cray, I. 1978. Slag/metal interaction, oxygen and toughness in submerged arc welding. *Welding Journal* 57: 63–75.
6. Chai, C. S., and Eagar, T. W. 1982. Slag metal reactions in binary CaF₂ — metal oxide welding fluxes. *Welding Journal* 61(7): 229–232.
7. Indacochea, J. E., Blander, M., Christensen, N., and Olson, D. L. 1985. Chemical reactions during submerged arc welding with FeO — MnO — SiO₂ fluxes. *Metallurgical Transactions B*, Vol. 16 B, pp. 237–245.
8. Mitra, U., and Eagar, T. W. 1984. Slag metal reactions during submerged arc welding of alloy steels. *Metallurgical Transactions A*, Vol. 15A, pp. 217–227.
9. Mitra, U., and Eagar, T. W. 1991. Slag metal reactions during welding, Part III, verification of the theory. *Metallurgical Transactions B*, pp. 83–100.
10. Lau, T., Weatherly, G. C., and Mclean, A. 1985. The source of oxygen and nitrogen contamination in submerged arc welding using CaO-Al₂O₃-based fluxes. *Welding Journal* 64(12): 343–347.
11. Natalie, C. A., Olson, D. L., and Blander, M. 1990. Weld-pool pyrometallurgy. *Welding: Theory and Practice*, Ed. D. L. Olson,

— continued on page 146-s

Appendix 1 — Standard Error, t Statistic, Level of Significance and Confidence Interval for the Responses (Dependent Variables)

Response: Weld Metal Delta Oxygen (ΔO_2) Content

Effect	Std. Error	t Statistic	P Significance	Confidence Interval (95%)	
				Lower	Upper
CaO	6.651202	8.86032	0.00000	45.6362	72.22735
MgO	9.177225	-1.87863	0.064999	-35.5856	1.10441
CaF ₂	2.708845	0.97910	0.331337	-2.7627	8.06713
Al ₂ O ₃	3.385175	3.77529	0.000360	6.0131	19.54688
CaO.MgO	0.272755	-3.33137	0.001460	-1.4539	-0.36342
CaO.CaF ₂	0.193945	-7.94330	0.000000	-1.9282	-1.15287
MgO.CaF ₂	0.248777	3.44178	0.001040	0.3589	1.35354
CaO.Al ₂ O ₃	0.211295	-9.66250	0.000000	-2.4640	-1.61926
MgO.Al ₂ O ₃	0.264115	3.01597	0.003711	0.2686	1.32452
CaF ₂ .Al ₂ O ₃	0.175454	2.08681	0.041024	0.0154	0.71687

Response: Weld Metal Delta Manganese (ΔMn) Content

Effect	Std. Error	t Statistic	P Significance	Confidence Interval (95%)	
				Lower	Upper
CaO	0.006001	-4.97699	0.000005	-0.041862	-0.017871
MgO	0.008280	6.73601	0.000000	0.039223	0.072326
CaF ₂	0.002444	-1.76890	0.081829	-0.009209	0.000562
Al ₂ O ₃	0.003054	-0.72955	0.468413	-0.008334	0.003877
CaO.MgO	0.000246	-1.92738	0.058517	-0.000966	0.000018
CaO.CaF ₂	0.000175	7.00053	0.000000	0.000875	0.001575
MgO.CaF ₂	0.000224	-6.02449	0.000000	-0.001801	-0.000904
CaO.Al ₂ O ₃	0.000191	7.14100	0.000000	0.000980	0.001742
MgO.Al ₂ O ₃	0.000238	-6.42759	0.000000	-0.002008	-0.001055
CaF ₂ .Al ₂ O ₃	0.000158	1.28571	0.203325	-0.000113	0.000520

Response: Weld Metal Delta Silicon (ΔSi) Content

Effect	Std. Error	t Statistic	P Significance	Confidence Interval (95%)	
				Lower	Upper
CaO	0.004538	2.68324	0.009336	0.003105	0.021247
MgO	0.006261	8.88579	0.000000	0.043119	0.068151
CaF ₂	0.001848	3.41049	0.001146	0.002609	0.009997
Al ₂ O ₃	0.002310	5.87068	0.000000	0.008942	0.018175
CaO.MgO	0.000186	-7.32795	0.000000	-0.001736	-0.000992
CaO.CaF ₂	0.000132	-0.47717	0.634916	-0.000328	0.000201
MgO.CaF ₂	0.000170	-7.84564	0.000000	0.001671	-0.000992
CaO.Al ₂ O ₃	0.000144	-1.31626	0.192834	-0.000478	0.000098
MgO.Al ₂ O ₃	0.000180	-7.92859	0.000000	-0.001789	-0.001068
CaF ₂ .Al ₂ O ₃	0.0000120	1.83448	0.071365	-0.000020	0.000459

Response: Weld Metal Delta Sulphur (ΔS) Content

Effect	Std. Error	t Statistic	P Significance	Confidence Interval (95%)	
				Lower	Upper
CaO	0.000495	5.91035	0.000000	0.001937	0.003917
MgO	0.000683	6.87823	0.000000	0.003334	0.006066
CaF ₂	0.000202	8.13973	0.000000	0.001239	0.002045
Al ₂ O ₃	0.000252	8.22036	0.000000	0.001568	0.002576
CaO.MgO	0.000020	-7.83173	0.000000	-0.000200	-0.000118
CaO.CaF ₂	0.000014	-4.86116	0.000008	-0.000099	-0.000041
MgO.CaF ₂	0.000019	-5.53316	0.000001	-0.000140	-0.000065
CaO.Al ₂ O ₃	0.000016	-5.03865	0.000004	-0.000111	-0.000048
MgO.Al ₂ O ₃	0.000020	-6.03380	0.000000	-0.000158	-0.000079
CaF ₂ .Al ₂ O ₃	-0.000019	-1.48386	0.142913	-0.000045	0.000007

Response: Weld Metal Delta Carbon (ΔC) Content

Effect	Std. Error	t Statistic	P Significance	Confidence Interval (95%)	
				Lower	Upper
CaO	0.001039	-1.64773	0.104468	-0.004399	0.000365
MgO	0.001433	5.06798	0.000004	0.004399	0.010129
CaF ₂	0.000423	3.01568	0.003714	0.000430	0.002121
Al ₂ O ₃	0.000529	-0.81781	0.416599	-0.001489	0.000624
CaO.MgO	0.000043	-2.93944	0.004615	-0.000210	-0.000040
CaO.CaF ₂	0.000030	2.38676	0.020062	0.000012	0.000133
MgO.CaF ₂	0.000039	-4.96770	0.000006	-0.000271	-0.000115
CaO.Al ₂ O ₃	0.000033	5.25772	0.000002	0.000108	0.000239
MgO.Al ₂ O ₃	0.000041	-4.41123	0.000042	-0.000264	-0.000100
CaF ₂ .Al ₂ O ₃	0.000027	0.93231	0.354781	-0.000080	0.000029

Appendix 2 — Text of Whole Mixture Model for the Responses (Dependent Variables)

Dependent Variable	R ²	SS Model	df Model	MS Model	SS Residual	df Residual	MS Residual	F Value	P Significance
Delta O ₂	0.686865	467971.5	9	51996.84	213343.9	62	3441.031	15.11083	0.000000
Delta Mn	0.648355	0.370643	9	0.041183	0.201023	62	0.003242	12.70159	0.000000
Delta Si	0.682053	0.212610	9	0.023623	0.099110	62	0.001599	14.77791	0.000000
Delta S	0.382705	0.005212	9	0.000579	0.008406	62	0.000136	4.270905	0.000242
Delta C	0.528908	0.006010	9	0.000668	0.005353	62	0.000086	7.734355	0.000000
Oxygen content	0.680338	476622.7	9	52958.02	223945.3	62	3612.02	14.66162	0.000000

Appendix 3 — Standard Error, t Statistic, Level of Significance, and Confidence Interval for the Responses

Effect	Std. Error	t Statistic	P Significance	Confidence Interval (95%)	
				Lower	Upper
CaO	6.814592	9.28970	0.000000	49.6834	76.92770
MgO	9.402668	-1.32095	0.191373	-32.2161	6.37522
CaF ₂	2.775389	2.32653	0.023273	0.9061	12.00495
Al ₂ O ₃	3.468333	4.83663	0.000009	9.8420	23.70816
CaO.MgO	0.279456	-3.38446	0.001241	-1.5044	-0.38718
CaO.CaF ₂	0.198709	-7.83541	0.000000	-1.9542	-1.15975
MgO.CaF ₂	0.254888	3.27729	0.001720	0.3258	1.34486
CaO.Al ₂ O ₃	0.216486	-9.52158	0.000000	-2.4940	-1.62854
MgO.Al ₂ O ₃	0.270603	2.83515	0.006177	0.2263	1.30813
CaF ₂ .Al ₂ O ₃	0.179764	2.10640	0.039224	0.0193	0.73800

— continued from page 144-s

R. Dixon, and A. L. Liby, chapter 5, Elsevier Science publishers, B.V., pp. 151–173.

12. Moor, M. A. B., North, T. H., and Bell, H. B. 1978. Characteristic properties of flux formulations used in submerged arc welding. *Welding and Metal Fabrication*, (4): 193–199.

13. Eagar, T. W. Oxygen and nitrogen contamination during arc welding. *Weldments: Physical Metallurgy and Failure Phenomena*, also E. J. Charistofel, et al., p. 31, Schenectady, N. Y., General Electric Co.

14. Schwemmer, D. D., Olson, D. L., and Williamson, D. L. 1979. The relationship of weld penetration to the welding flux. *Welding Journal* 58(5): 153-s to 160-s.

15. Mills, K. C., and Keene, B. J. 1981. Physicochemical properties of molten CaF₂-based slags. *International Metals Review*, No. 1, pp. 21–69.

16. Indacochea, J. E., and Olson, D. L. 1983. Relationship of weld metal microstructure and penetration to weld metal oxygen content. *Journal Materials for Energy Systems*, ASM International, Vol. 5, No. 3, pp. 139–148.

17. Polar, A., Indacochea, J. E., and Blander, M. 1990. Electrochemically generated oxygen contamination in submerged arc welding. *Welding Journal* 69(2): 68–74.

18. Chai, C. S., and Eagar, T. W. 1981. Slag-metal equilibrium during submerged arc welding. *Metallurgical Transactions B*, Vol. 12B, (9): 539–547.

19. Polar, A., Indacochea, J. E., and Blander, M. 1991. Fundamentals of the chemi-

cal behavior of select welding fluxes. *Welding Journal* 70(1): 15–19.

20. Indacochea, J. E., Blander, M., and Shah, S. 1989. Submerged arc welding: Evidence for electrochemical effects on the weld pool. *Welding Journal* 68(3): 77–83.

21. Kim, J. H., Frost, R. H., Olson, D. L., and Blander, M. 1990. Effect of electrochemical reactions on submerged arc weld metal compositions. *Welding Journal* 69(12): 446–453.

22. Blander, M., and Olson, D. L. 1986. Electrochemical effects on weld pool chemistry in submerged arc and D.C. electroslag welding. *Proceedings of the International Conference on Trends in Welding Research*, Gatlinburg, Tenn., ASM International, 8605-007, pp. 363–366.

23. Dallam, C. B., Liu, S., and Olson, D. L. 1985. Flux composition dependence of microstructure and toughness of submerged arc HSLA weldments. *Welding Journal* 64(5): 140–150.

24. Dunn, P. S., Natalie, C. A., and Olson, D. L. 1986. Sol-gel fluxes for flux cored welding consumables. *Journal of Materials for Energy Systems*. Vol. 8, No. 2, pp. 176–184.

25. Burck, P. A., Indacochea, J. E., and Olson, D. L. 1990. Effects of welding flux additions on 4340 steel weld metal composition. *Welding Journal* 69(3): 115–122.

26. Mclean, R. A., and Anderson, V. L. 1966. Extreme vertices design of mixture experiments. *Technometrics*, Vol. 8, pp. 447–454.

27. Snee, R. D., and Marquardt, D. W. 1976. Screening concepts and designs for experiments with mixture. *Technometrics*, Vol. 18, pp. 19–29.

28. Snee, R. D., and Marquardt, D. W. 1974.

Extreme vertices designs for linear mixture models. *Technometrics*, Vol. 16, pp. 399–408.

29. Snee, R. D. 1979. Experimental designs for mixture systems with multicomponent constraints. *Communications in Statistics: Theory and Methods*, Vol. A8, No. 4, pp. 303–326.

30. Moore, J. J. *Chemical Metallurgy*, Chapter 5, slag chemistry, 2nd edition, pp. 152–172.

31. Surian, E. 1997. ANSI/AWS E7024 SMAW Electrodes: The effect of coating magnesium additions. *Welding Journal* 76(10): 404–411.

32. Dean, J. A. *Langes Handbook of Chemistry*, formerly compiled and edited by N. A. Langi, thirteenth edition, McGraw Hill Book Co., Sec. 9: 13–14, Sec 4, pp. 15, 35, and 71.

33. Davis, M. L. E., and Bailey, N. 1991. Evidence from inclusion chemistry of element transfer during submerged arc welding. *Welding Journal* 70(2): 57–66.

34. Oiks, G. Converter and open hearth steel manufacture. *Fundamentals of Theory and Technology*, MIR Publishers, Moscow, pp. 97–200, 324–334.

35. Herasymanko, P., and Speight, G. E. 1950. Ionic theory of slag metal equilibria, Part-II, applications to the basic, open hearth process. *Journal of Iron and Steel Institute*, (12): 289–303.

36. Cornell, J. A. *Experiments with Mixtures, Designs, Models and the Analysis of Mixture Data*, John Wiley & Sons, Chapter 3, The use of independent variables, pp. 65–109.